Electronic Supplementary Material (ESI) for Physical Chemistry Chemical Physics.

Supporting Information:

Kinetics of the Reaction of $CO_3^-(H_2O)_n$, n = 0, 1, 2, with Nitric Acid, a Key Reaction in Tropospheric Negative Ion Chemistry

Christian van der Linde,[*a] Wai Kit Tang,[b] Chi-Kit Siu[*b] and Martin K. Beyer[*a]

[a] *Institut für Ionenphysik und Angewandte Physik, Universität Innsbruck, Technikerstraße 25, 6020 Innsbruck, Austria*

E-Mail: christian.van-der-linde@uibk.ac.at; martin.beyer@uibk.ac.at

[b] *Department of Chemistry, City University of Hong Kong, 83 Tat Chee Avenue, Kowloon Tong, Hong Kong SAR, P. R. China*

E-mail: chiksiu@cityu.edu.hk

Table S1: Comparison of methods/basis sets with experimental values.

Binding Energy / kJ mol^{-1}	**M06-2X**			**CCSD(T)//M06-2X[a]**		**B3LYP**		**MP2**		**Experiment**
Basis Sets [a]	**BS1**	**BS2**	**BS3**	**BS2**	**BS3**	**BS1**	**BS3**	**BS1**	**BS3**	
$\Delta H_0°$										
NO_3^- + H_2O	65	62	60	60	59	58	52	61	59	61.09 ± 0.84 [c]
$NO_3^-(H_2O)$ + H_2O	58	54	52	53	52	50	45	52	51	59.8 [c]
$CO_3^{\bullet-}$ + H_2O	62	59	58	56	56	50	46	43	39	58.99 ± 0.84 [d]
$CO_3^{\bullet-}(H_2O)$ + H_2O	53	50	49	48	48	44	40	64	68	56.9 [d]
$CO_3^{\bullet-}$+ HNO_3	144	143	141	130	128	118	116	108	109	
$\Delta G_{298}°$										
NO_3^- + H_2O	37	34	33	32	31	28	22	36	29	30.1 ± 1.3 [c]
$NO_3^-(H_2O)$ + H_2O	27	23	21	22	20	20	11	15	17	22
$CO_3^{\bullet-}$ + H_2O	29	27	26	24	23	22	16	12	7	27.6 ± 1.7 [d]
$CO_3^{\bullet-}(H_2O)$ + H_2O	21	17	16	15	15	11	8	31	35	19.9
$CO_3^{\bullet-}$+ HNO_3	103	102	100	88	87	79	78	108	70	

[a] BS1: 6-311++G(d,p); BS2: 6-311++(3df,3pd); BS3: Aug-cc-pVTZ

[b] Single-point energies at CCSD(T)//M06-2X level include zero-point correction evaluated at M06-2X level.

[c] Lee, N.; Keesee, R.G.; Castleman, A.W., Jr., The properties of clusters in the gas phase. IV. Complexes of H_2O and HNO_x clustering on NO_x-, J. Chem. Phys., 1980, 72, 1089.

[d] Keesee, R.G.; Lee, N.; Castleman Jr., Properties of Clusters in the Gas Phase. 3. Hydration Complexes of CO_3^- and HCO_3^-, J. Am. Chem. Soc., 1979, 101, 10, 2599.

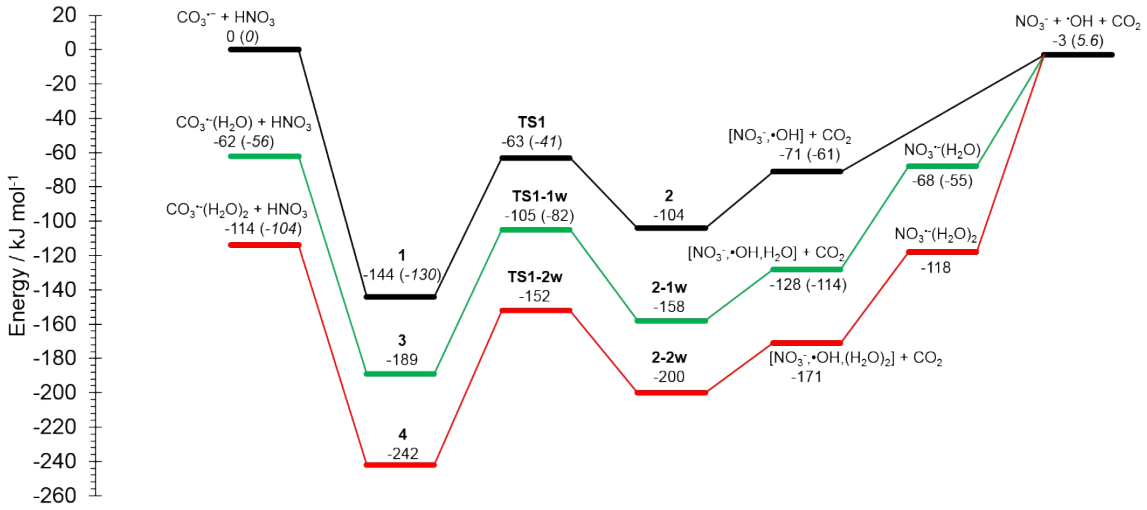

Figure S1: Influence of solvation. Calculated at M06-2X/6-311++G(d,p)/*(CCSD(T)//M06-2X/6-311++G(3df,3pd) with zero point correction evaluated at M06-2X/6-311++G(3df,3pd) level in parentheses).*

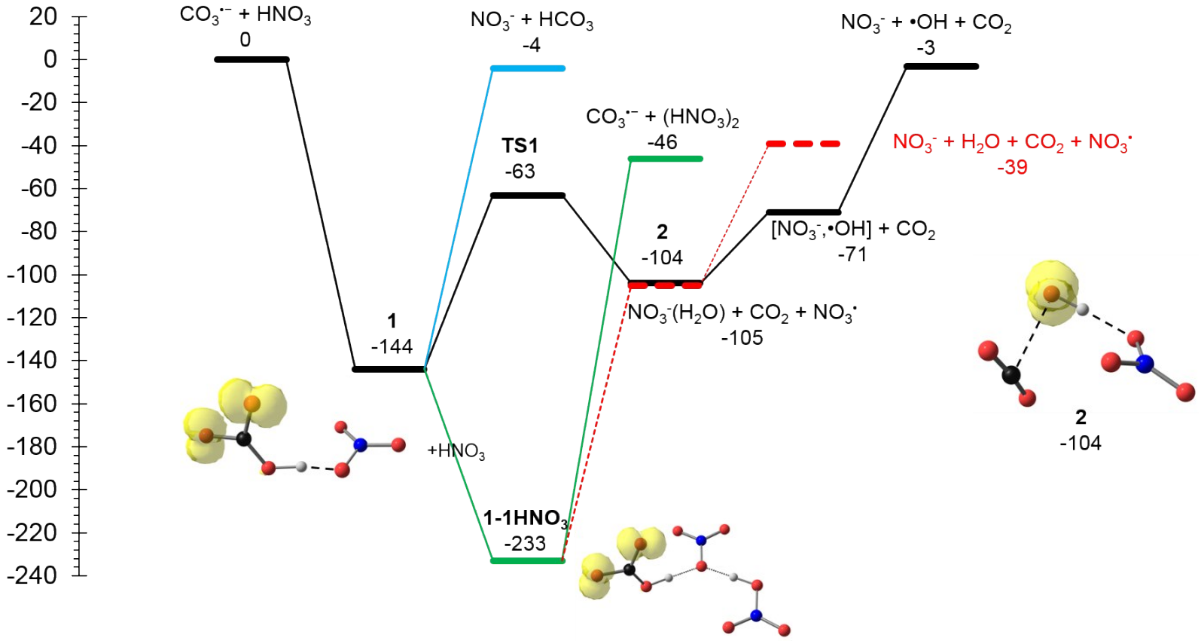

Figure S2: PES of $CO_3^{\bullet-}$ + HNO_3 including all possible reaction channels. Calculated at M06-2X/6-311++G(d,p) level of theory, with zero-point corrected energies given in kJ mol^{-1}.

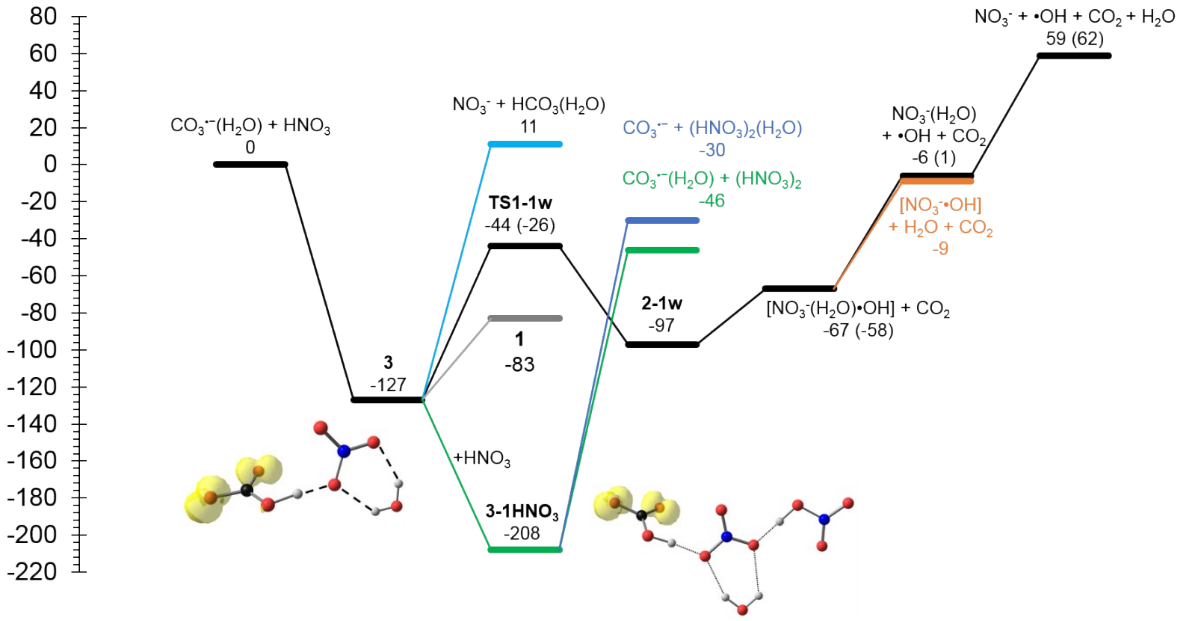

Figure S3: PES of $CO_3^-(H_2O)$ + HNO_3 including all possible reaction channels. Calculated at M06-2X/6-311++G(d,p) level of theory, with zero-point corrected energies given in kJ mol^{-1}.

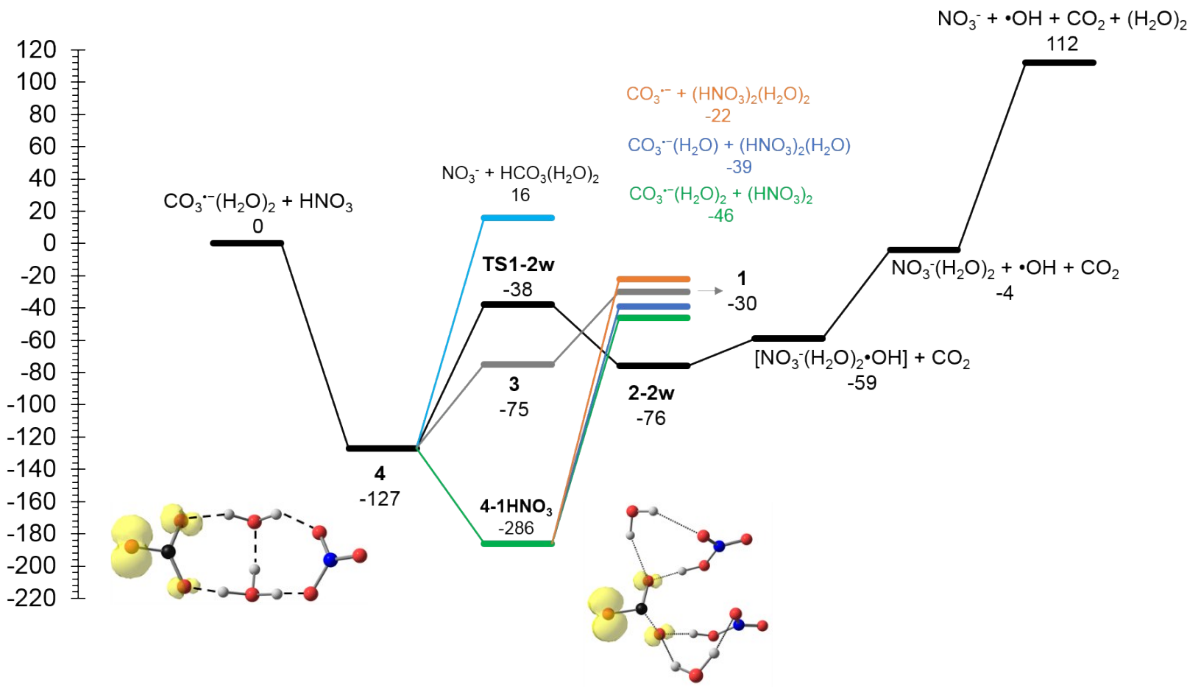

Figure S4: PES of $CO_3^-(H_2O)_2$ + HNO_3 including all possible reaction channels. Calculated at M06-2X/6-311++G(d,p) level of theory, with zero-point corrected energies given in kJ mol^{-1}.

Mass Spectra (Figures S1-S3)

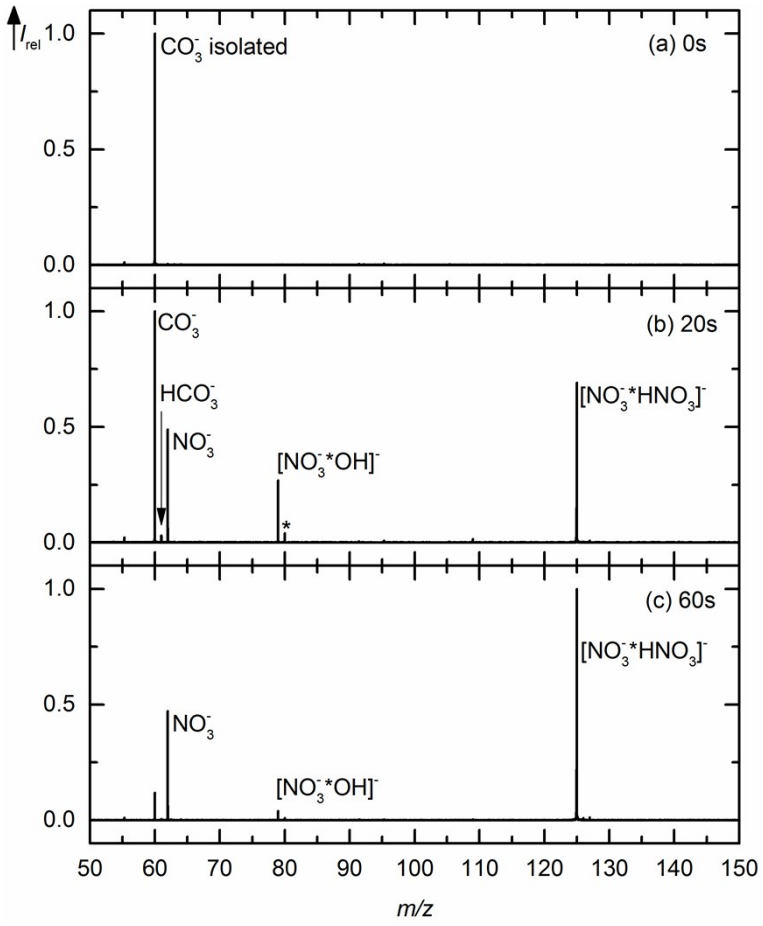

Figure S5: Mass spectra of the reaction of CO_3^- with HNO_3 at a reactant pressure of 1.4×10^{-8} mbar after different reaction delays of (a) 0s, (b) 20s and (c) 60s.

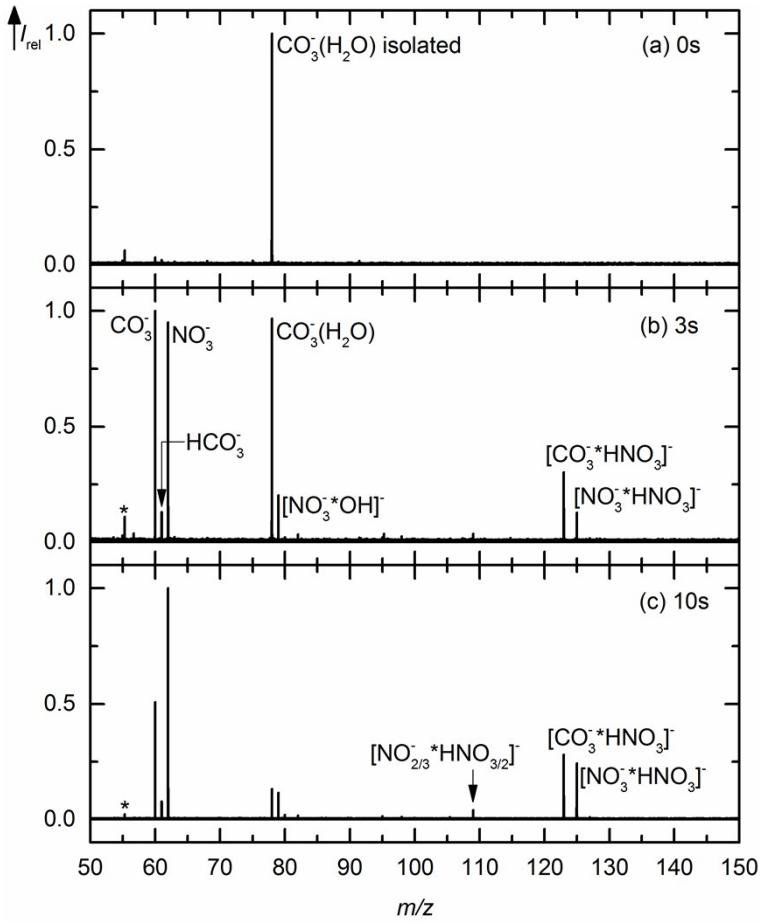

Figure S6: Mass spectra of the reaction of $CO_3^-(H_2O)$ with HNO_3 at a reactant pressure of 2.1×10^{-8} mbar after different reaction delays of (a) 0s, (b) 3s and (c) 10s.

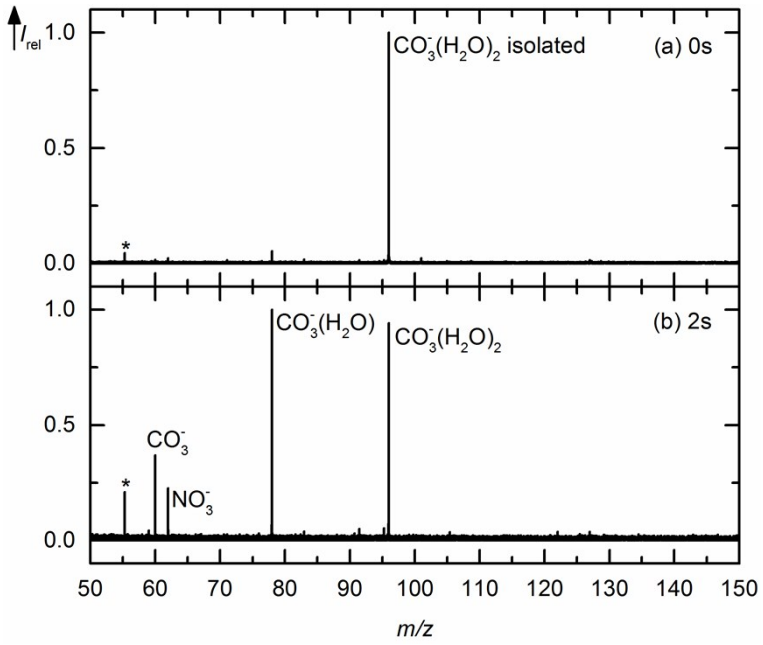

Figure S7: Mass spectra of the reaction of $CO_3^-(H_2O)_2$ with HNO_3 at a reactant pressure of 2.1×10^{-8} mbar after different reaction delays of (a) 0s and (b) 2s.

Kinetic Analysis

For the kinetic analysis a pseudo-first-order rate law can be used. This approximation is valid, if the concentration of one reactant is considerably larger than of the other reactant. The experiments performed in the ICR fulfill this condition. The pressure of the reactant is constant with a density of typically 10^9 cm^{-3}. The cluster density is in the range of 10^6 cm^{-3}.

For a bimolecular reaction A + B → P a second order rate law (SI-1) is valid.

$$\frac{dN_A}{dt} = -k_{abs} N_A N_B \qquad \text{(SI-1)}$$

If one of the concentrations of A and B is considerably larger than that of the second reaction partner ($N_A << N_B$), it can be treated as constant. The rate law (SI-1) can be simplified to equation (SI-2) with $k_{rel} = k_{abs} N_B$.

$$\frac{dN_A}{dt} = -k_{rel} N_A \qquad \text{(SI-2)}$$

The measured intensities I_A are directly proportional to the concentration of the reactant N_A ($I_A \propto N_A$) and can be used for further data evaluation, equation (2.6).

$$\frac{dI_A}{dt} = -k_{rel} I_A \qquad \text{(SI-3)}$$

The rate law in equation (SI-3) is only valid for a simple reaction A + B → P. To describe complex reaction networks with consecutive and parallel reactions, a more complex approach is necessary. The following equation with n coupled differential equations (SI-4) is typically used to describe such systems.

$$\frac{\partial \vec{I}}{\partial t} = K\vec{I} = \begin{pmatrix} k_{11} & \cdots & k_{1n} \\ \vdots & \ddots & \vdots \\ k_{n1} & \cdots & k_{nn} \end{pmatrix} \begin{pmatrix} I_1 \\ \vdots \\ I_n \end{pmatrix} \qquad \text{(SI-4)}$$

The matrix ***K*** contains the n^2 rate constants k_{ij} of the reaction system. The vector $\vec{I}$ contains the intensities of the n species in the reaction system. For a small time interval $\Delta t = t_2 - t_1$ the differential quotient in (SI-4) can be approximated by (SI-5)

$$\frac{\vec{I}(t_2) - \vec{I}(t_1)}{\Delta t} = K\vec{I}(t_1) \qquad \text{(SI-5)}$$

After rearrangement of this equation (SI-5) the intensities $\vec{I}(t_2)$ can be directly calculated. Using the identity matrix ***E*** ,equation (SI-6) is obtained.

$$\vec{I}(t_2) = (K\,\Delta t + E)\vec{I}(t_1) \qquad \text{(SI-6)}$$

This equation (SI-6) allows to fit the intensity-time charts numerically. The relative rate constants k_{rel}/ s^{-1} can be obtained, and converted to absolute rate k_{abs}/ cm^3 s^{-1} constants using equation (SI-7).

$$k_{abs} = \frac{k_{rel}}{\rho} \tag{SI-7}$$

Using $\rho = N/V$, the ideal gas law $pV = Nk_BT$ and a factor K_p for pressure correction the expression (SI-8) is obtained for k_{abs} .

$$k_{abs} = K_p \frac{k_{rel} k_B T}{p_x^{gauge}} \tag{SI-8}$$

The intensity-time charts can be fitted using equation (SI-6). This fit is implemented in the software Analyzze using a genetic algorithm for optimization. The fit needs the intensities at $t = 0$ and the allowed reaction channels as start parameters. The fit also allows to distinguish between different isomers or ion distributions of e. g. different temperatures.

The genetic algorithm belongs to the group of evolutionary algorithms (EA). Such algorithms are well suited for complex problems without exact mathematical solutions. The principle of these algorithms is comparable to biological evolution. A set of possible solutions is tested against a set of rules, and the best results are selected. The selected solutions are called survivors. New possible solutions are added by mutations and cross-overs and tested again. The probability for mutations and cross overs can be adjusted in the fit parameters. The different solutions are optimized for the problem with each new cycle and match the quality criterion better and better.

Pressure Correction

An aqueous 70% HNO_3 solution is close to the azeotropic point and the chemical composition in the gas phase is therefore close to 70% HNO_3 and 30% water. As the cold cathode pressure gauge shows different sensitivity toward HNO_3 and H_2O, the measured pressure was corrected taking the different sensitivity into account. The pressure readout from the cold cathode pressure gauge is usually corrected using the following equation.[SI-1]

$$p_x^{cell} = \frac{G}{R_x} p_x^{gauge} = \frac{1}{K_p} p_x^{gauge} = \frac{G}{0.36\alpha_x + 0.30} p_x^{gauge} \tag{SI-9}$$

The parameter *G* represents an experimental geometry correction factor for the used instrument, R_x is the sensitivity towards different gases, being related to the polarizability of the gas α_x. p^{cell} is the actual pressure in the ICR cell while p^{gauge} represents the uncorrected pressure readout of the cold cathode.

To correct the pressure for two different gases being present in the UHV at the same time this correction procedure has to be modified. The uncorrected pressure readout can be described by the following equation:

$$p_{HNO_3+H_2O}^{gauge} = p_{HNO_3+H_2O}^{cell}\left(0.7\frac{0.36\alpha_{HNO_3}+0.30}{G}+0.3\frac{0.36\alpha_{H_2O}+0.30}{G}\right) \qquad \text{(SI-10)}$$

The correction factors are weighted by the chemical composition of the gas phase. After rearrangement of (SI-2) the corrected cell pressure can be calculated via (SI-11).

$$p_{HNO_3+H_2O}^{cell} = \frac{p_{HNO_3+H_2O}^{gauge} G}{0.7\left(0.36\alpha_{HNO_3}+0.30\right)+0.3\left(0.36\alpha_{H_2O}+0.30\right)} \qquad \text{(SI-11)}$$

The geometry factor *G* has the experimental value of (3.7±1.0), the polarizability of HNO_3 is $\alpha(HNO_3)$ = 3.55 Å³ and for water $\alpha(H_2O)$ = 1.45 Å³. The HNO_3 partial pressure was taken as 70% of the corrected total pressure $p_{HNO_3+H_2O}^{cell}$.

[SI-1] J. E. Bartmess, R. M. Georgiadis, *Vacuum* **1983**, *33*, 149–153.
[SI-2] Ed. D. R. Lide*, CRC Handbook of Chemistry and Physics*, **1995**, *75th Ed*., CRC Press, Boca Raton et al.

Rate Coefficient Matrix

The rate coefficient matrices (Table S1-S3) used for the fits in Figures 2-4 are shown on the following page. The species in the top row react to the species in the left column. Indices a,b correspond to two isomers/fractions that were used to describe the same m/z in the fit. *Init Int.* is the intensity of the corresponding species at t = 0s

Peak Assignments

#45.992	NO_2^-	#79.996	$[NO_3,H_2O]^-$
#59.984	CO_3^-	#96.006	$CO_3^-(H_2O)_2$
#60.991	HCO_3^-	#108.986	$[NO_3,HNO_2]^-$ or $[NO_2,HNO_3]^-$
#61.987	NO_3^-	#122.978	$[CO_3,HNO_3]^-$
#77.994	$CO_3(H_2O)^-$	#124.981	$[NO_3,HNO_3]^-$
#78.989	$[NO_3,OH]^-$		

Stability Analysis

The stability of all fit parameters was tested. These include the initial intensities and the relative rate coefficients k_{rel}. The tested parameter was changed in 5-10 steps by ±5% of its optimized value, and all other parameters were re-optimized. The resulting error was plotted against the value of the tested parameter. The resulting plots (Figures S8 and S9) are given with the rate coefficient matrix (Tables S1 and S2).

Table S1: Rate Coefficient Matrix for Figure 2.

Init Int.	0.0092	0.8835	0	0.0000	0.0051	0.0000	0.0002	0.0000	0.0017	0.1002
	45.992	59.984a	59.984b	60.991	61.987	78.989	79.996	108.986	124.981	electrons
45.992	0	0	0	0	0	0	0	0	0	0.2165
59.984a	0	0	0	0	0	0	0	0	0	0
59.984b	0	0	0	0	0	0	0	0	0	0
60.991	0	0.0020	0	0	0	0	0	0	0	0
61.987	2.4517	0.0071	0	0.0933	0	0	0	0	0.0000	0
78.989	0	0.0293	0	0	0	0	0	0	0	0
79.996	0	0	0	0	0	0.0180	0	0	0	0
108.986	0	0	0	0	0	0.0061	0.0994	0	0	0
124.981	0	0	0	0	0	0.1232	0.0000	0.3541	0	0
electrons	0	0	0	0	0	0	0	0	0	0

Table S2: Rate Coefficient Matrix for Figure 3.

Init Int.	0.0160	0.0289	0.0079	0.0062	0.2138	0.4301	0.0051	0.0033	0.0003	0.0066	0.2817
	45.992	59.984	60.991	61.987	77.994a	77.994b	78.989	108.986	122.978	124.981	electrons
45.992	0	0	0	0	0	0	0	0	0	0	0.1531
59.984	0	0	0	0	0	0.3508	0	0	0.0000	0	0
60.991	0	0.0000	0	0	0.0000	0.0385	0	0	0	0	0
61.987	0.7823	0.0000	0.0253	0	0	0.1945	0	0	0.0000	0.0157	0
77.994a	0	0	0	0	0	0	0	0	0	0	0
77.994b	0	0	0	0	0.1180	0	0	0	0	0	0
78.989	0	0.0474	0	0	0.0000	0.0726	0	0	0	0	0
108.986	0	0	0	0	0	0	0.0712	0	0	0	0
122.978	0	0	0	0	0.0484	0.0730	0	0	0	0	0
124.981	0	0	0	0	0	0	0.1929	0.1441	0.0000	0	0
electrons	0	0	0	0	0	0	0	0	0	0	0

Table S3: Rate Coefficient Matrix for Figure 4.

Init Int.	0.0151	0.0034	0.0198	0.0462	0.0000	0.0000	0.7053	0	0.2101
	45.992	59.984	61.987	77.994a	77.994b	78.989	96.006a	96.006b	electrons
45.992	0	0	0	0	0	0	0	0	0.2128
59.984	0	0	0	1.6593	0.1730	0	0	0	0
61.987	0.0000	0.0921	0	0.9902	0.0156	0	0	0	0
77.994a	0	0	0	0	0	0	0.0465	0	0
77.994b	0	0	0	0.0033	0	0	0.3874	0	0
78.989	0	0.0364	0	0.0000	0.0000	0	0.0000	0	0
96.006a	0	0	0	0	0	0	0	0	0
96.006b	0	0	0	0	0	0	0	0	0
electrons	0	0	0	0	0	0	0	0	0

Stability Analysis

Figure S8: Stability Test of Reaction Matrix from Figure 2 (see Table S1). The initial intensities for mass 79.996 and 108.986 are not well defined as these are products and do not appear in significant intensities at t=0s.

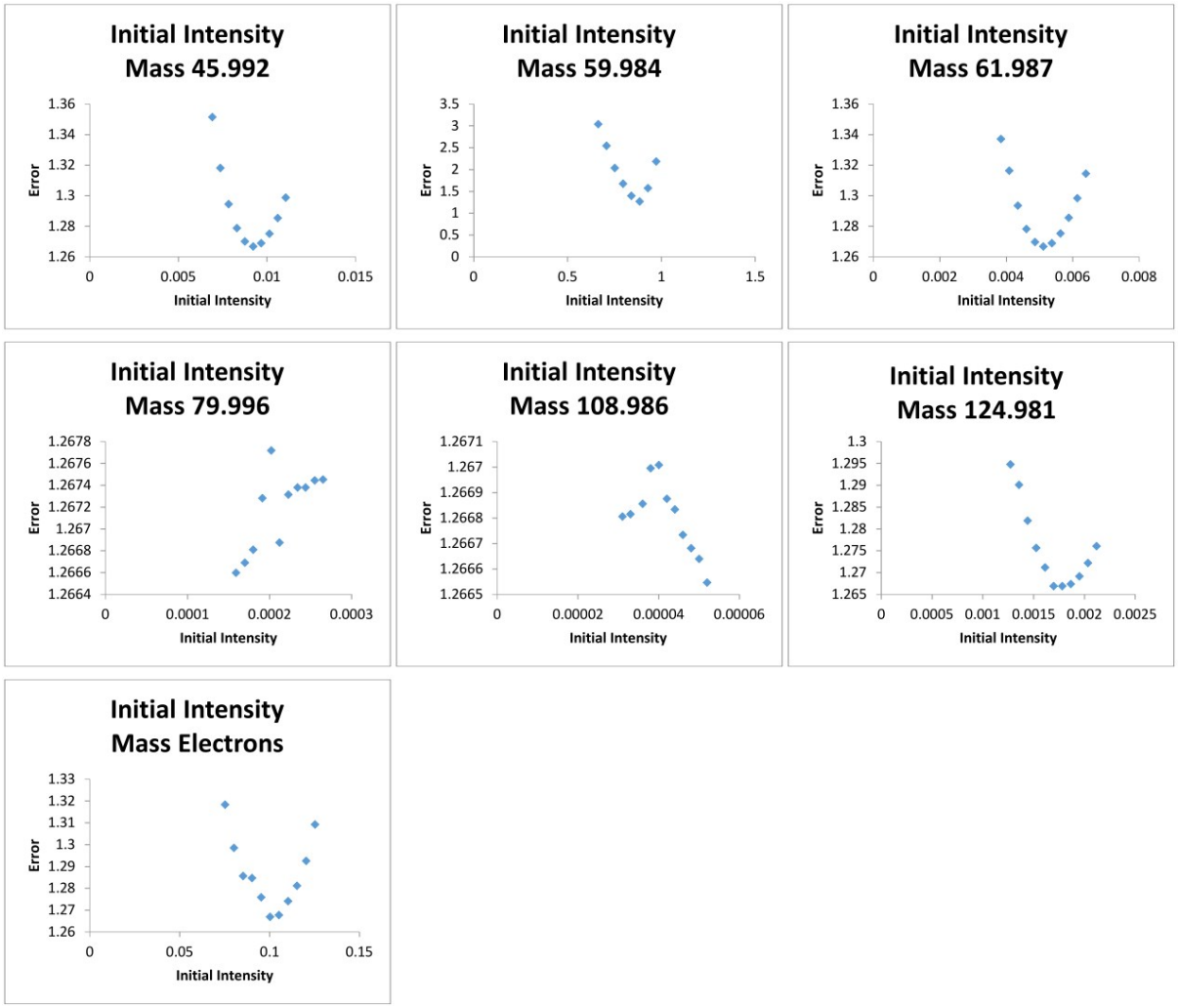

Figure S8: continued.

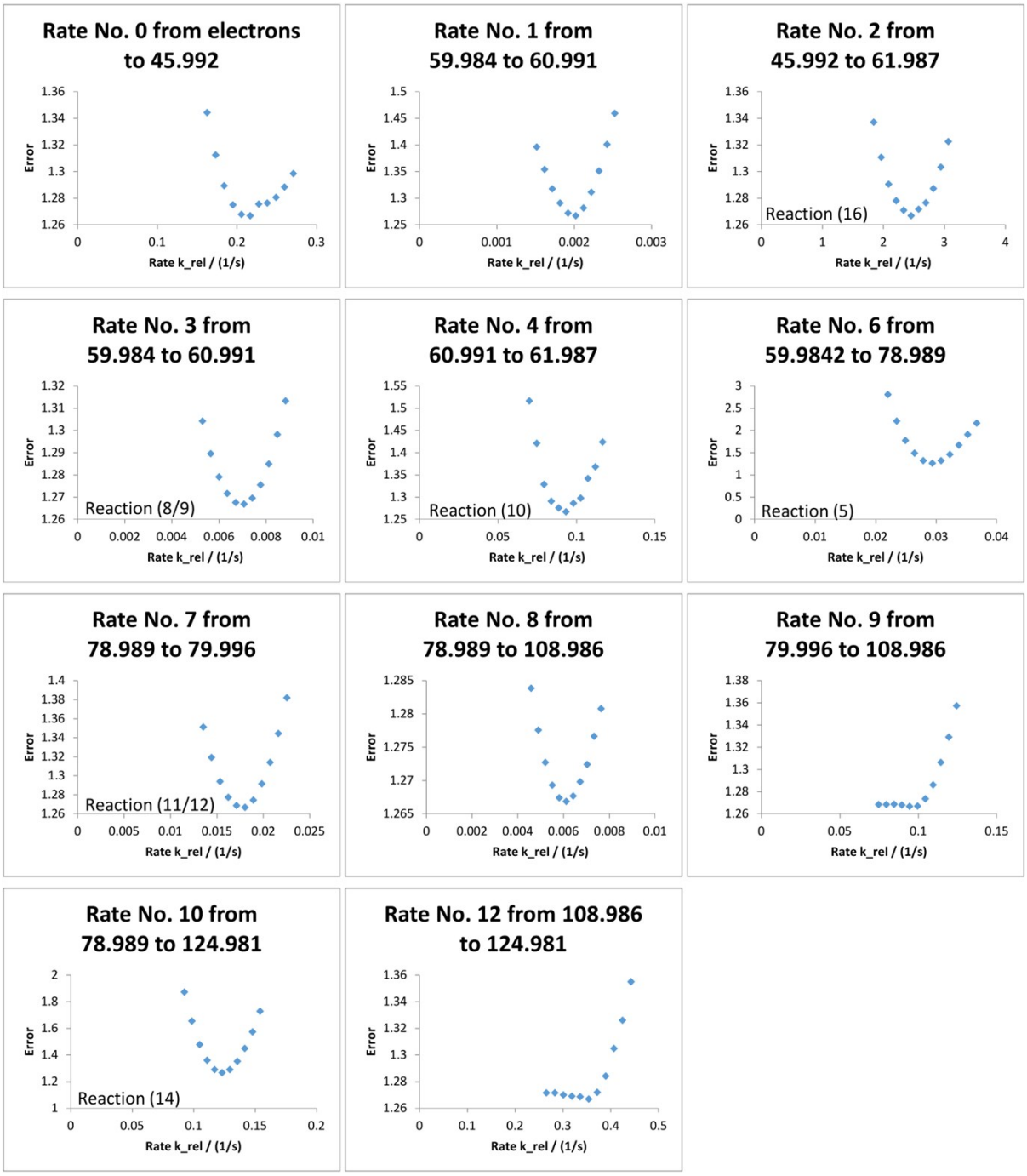

Figure S9: Stability Test of Reaction Matrix from Figure 3 (see Table S2).

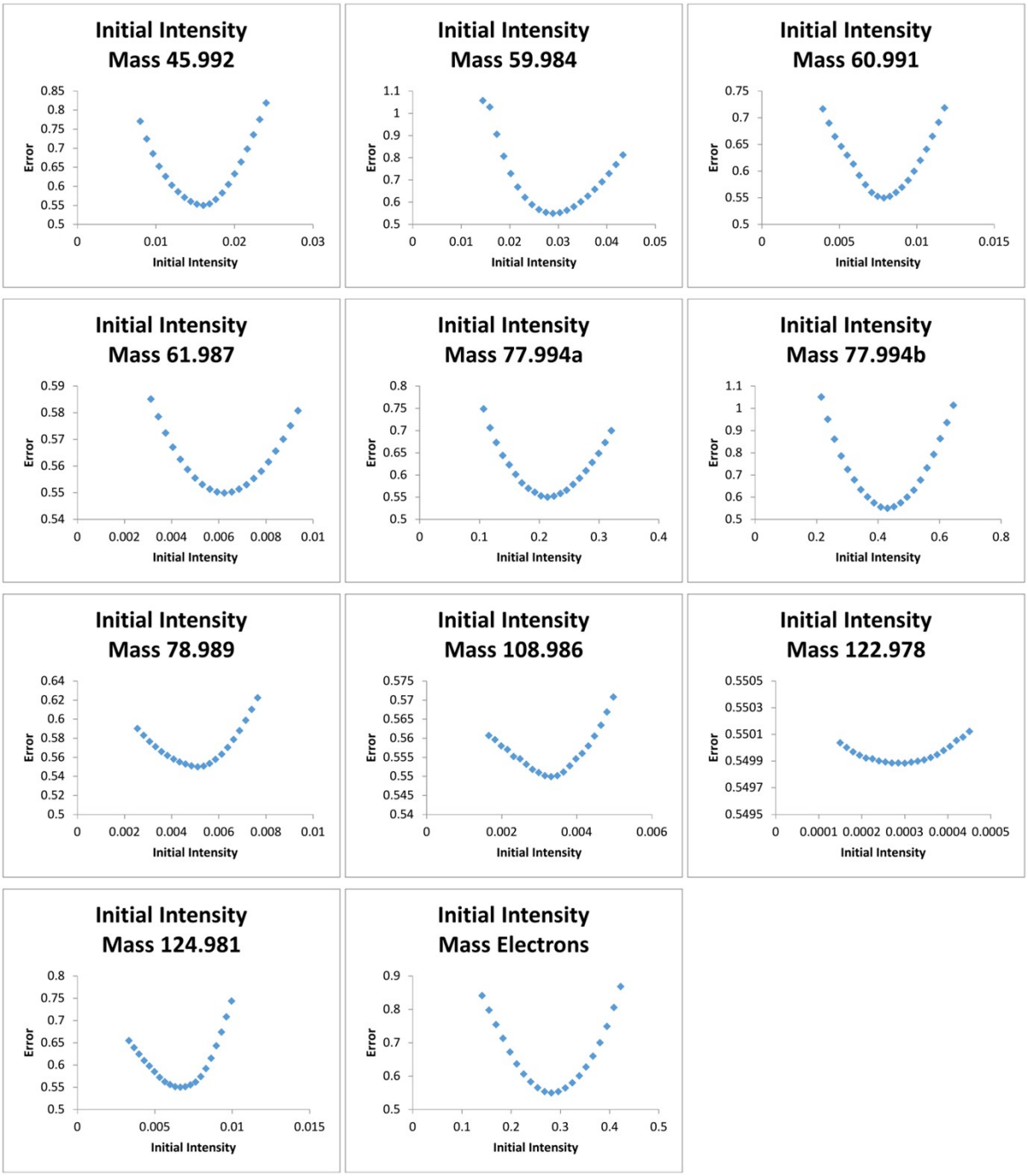

Figure S9: continued.

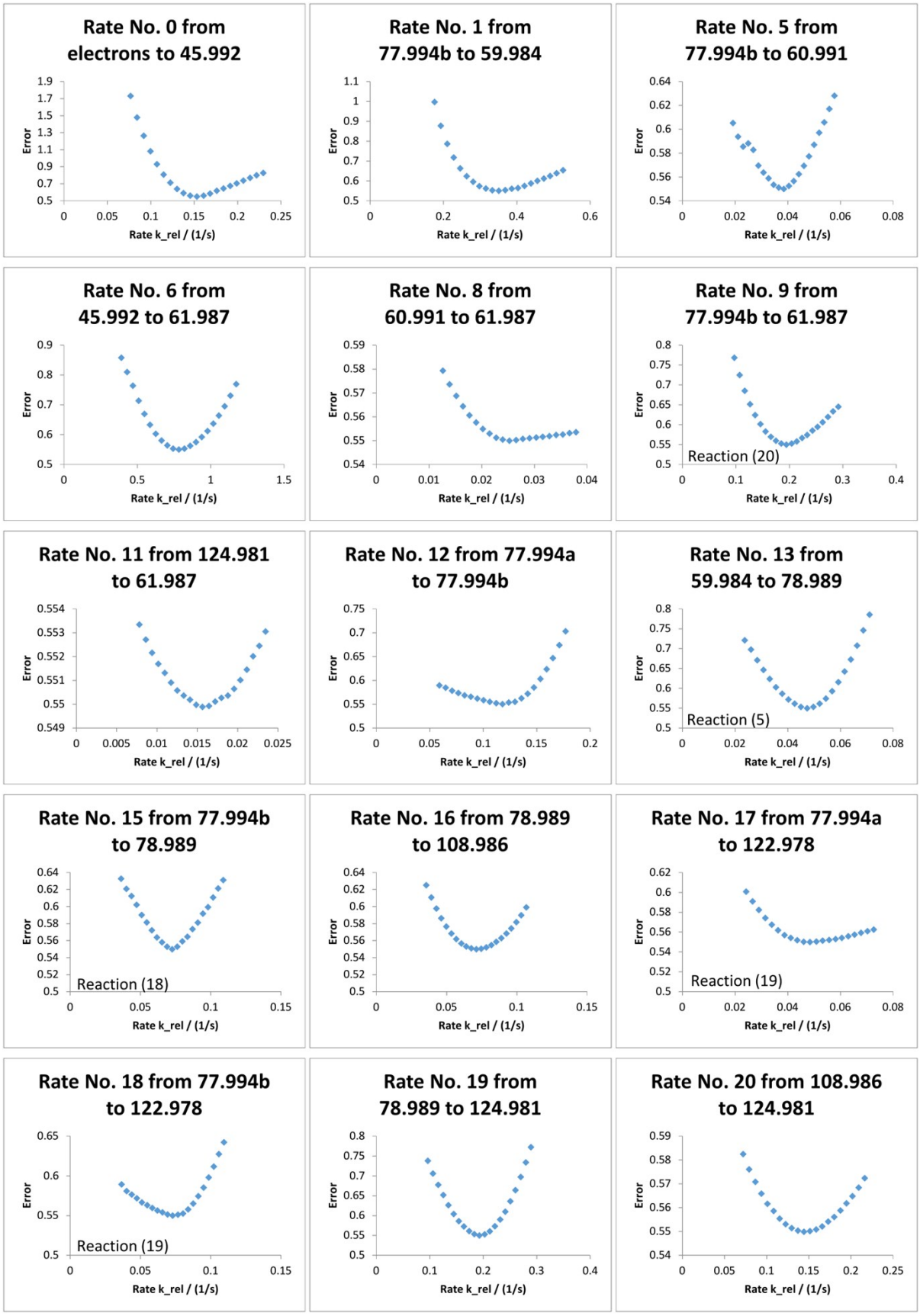

Table S4. Cartesian coordinates, harmonic vibration analyses (frequency in cm^{-1}, IR intensity in km mol^{-1}) and energies (E, E_{zpc}, H_{298}, G_{298} in au) of all optimized structures as shown Figure 1.

$CO_3^{\bullet-}$
C 0.000000 0.000000 0.072616
O 0.000000 0.000000 1.306737
O 0.000000 1.043593 -0.680600
O 0.000000 -1.043593 -0.680600

418.3, 0.2; 512.8, 45.9; 837.4, 35.9; 1032.8, 58.7;
1118.2, 4.7; 1635.4, 441.4;

-263.786155583 -263.773501 -263.769091 -263.799121

HNO_3
N -0.141761 0.034174 -0.000095
O -1.041670 -0.738556 0.000098
O -0.158423 1.235850 -0.000019
O 1.108791 -0.552028 -0.000130
H 1.722741 0.198652 0.001075

477.8, 147.2; 624.7, 10.0; 709.7, 0.9; 811.7, 13.0;
984.3, 182.4; 1370.0, 87.5; 1427.5, 326.3; 1829.5, 523.6;
3799.6, 137.4;

-280.862518738 -280.835102 -280.830698 -280.860788

Structure 1
N 1.930918 0.042848 -0.063709
O 3.082969 0.107643 0.335343
O 1.489513 0.738577 -0.970414
O 1.142867 -0.809091 0.504067
H -0.069774 -0.788430 0.015306
O -3.145982 0.022449 -0.318927
C -1.934612 -0.019237 0.037146
O -1.115191 -0.908945 -0.359861
O -1.684049 0.924856 0.835766

37.5, 0.3; 45.4, 0.5; 56.3, 0.5; 118.1, 0.0;
155.2, 3.5; 312.2, 197.8; 562.3, 222.0; 575.8, 207.8;
734.5, 2.1; 774.8, 114.4; 801.5, 34.6; 857.5, 11.9;
1028.5, 354.1; 1065.0, 1293.1; 1121.2, 28.1; 1241.5,
1764.8;
1372.7, 203.0; 1477.2, 63.1; 1603.1, 792.6; 1631.7,
1137.3;
1762.4, 525.1;

-544.703041862 -544.663551 -544.654704 -544.699628

Structure TS1
O -3.143487 -0.513799 -0.451486
O -1.026902 -0.741920 -0.131228
H 0.003108 -0.144682 0.392484
C 2.386404 0.004079 -0.129519
O 2.728655 -1.076990 0.226998
O 0.947084 0.290126 0.847949
O 2.555265 0.967767 -0.797411
N -2.099243 -0.023057 -0.056696
O -2.013970 1.110016 0.402865

-378.7, 1186.2; 21.6, 0.3; 39.8, 0.6; 49.7, 1.6;
83.2, 0.5; 96.6, 9.0; 272.1, 13.6; 448.6, 81.0;
611.0, 650.1; 732.4, 9.6; 747.7, 16.2; 785.3, 28.2;
857.5, 15.9; 1070.1, 1236.8; 1137.0, 93.0; 1204.2, 1721.4;
1370.8, 270.3; 1380.8, 52.8; 1613.3, 35.5; 1657.9, 1840.9;
2133.4, 841.6;

-544.669597158 -544.632433 -544.623256 -544.670101

Structure 2
O -2.619723 -0.749399 0.121407
O -1.435233 1.045579 0.277665
H 0.110175 1.635097 -0.098474
C 1.794741 -0.598183 0.233977
O 1.412520 -0.525940 1.323171
O 1.027272 2.010599 -0.240501
O 2.273172 -0.722744 -0.811467
N -1.574105 -0.145950 -0.112395
O -0.640493 -0.686140 -0.735103

35.0, 1.0; 56.9, 1.1; 72.8, 0.5; 93.1, 0.4;
121.8, 2.3; 133.7, 5.5; 168.9, 2.9; 220.2, 29.3;
641.0, 82.2; 660.9, 134.6; 675.8, 48.8; 738.3, 12.4;
746.9, 14.4; 852.4, 57.0; 874.1, 29.9; 1137.1, 21.1;
1411.3, 28.9; 1432.1, 622.4; 1537.8, 756.8; 2446.4, 806.9;
3195.2, 1106.5;

-544.687471926 -544.648170 -544.637915 -544.685729

Structure $[NO_3^-,{}^{\bullet}OH]$
N 0.752764 0.009203 0.000204
O 1.958721 -0.254993 -0.001284
O 0.348909 1.182999 0.000706
O -0.092507 -0.927669 0.001217
H -1.697146 -0.228153 0.000583
O -2.661649 0.020130 -0.000890

46.1, 0.7; 61.0, 0.5; 205.5, 23.6; 612.4, 93.6;
40.4, 1.7; 756.6, 7.4; 761.1, 118.2; 869.9, 22.8;
1135.0, 15.7; 1440.1, 716.0; 1525.4, 723.9; 3307.7,
1025.8;

-356.098835430 -356.072725 -356.066215 -356.103782

CO_2
C 0.000000 0.000000 0.000000
O 0.000000 0.000000 1.154777
O 0.000000 0.000000 -1.154777

687.8, 40.3; 687.8, 841.3; 1419.6, 0.0; 2468.7, 0.0;

-188.574879675 -188.562888 -188.559341 -188.583564

NO_3^-
N 0.000002 -0.000068 0.000771
O 1.204714 0.321941 -0.000225
O -0.881230 0.882071 -0.000225
O -0.323485 -1.203952 -0.000225

736.5, 0.0; 736.7, 0.0; 876.2, 14.1; 1134.9, 0.0;
1468.7, 687.2; 1470.5, 688.1;

-280.343402574 -280.328769 -280.324703 -280.354223

$HO^{\bullet}$
H 0.000000 0.000000 -0.864013
O 0.000000 0.000000 0.108002

3790.7, 0.0;

-75.726597263 -75.717961 -75.714657 -75.734882

$HCO_3^{\bullet}$
H 1.741979 0.539910 -0.002771
O 1.224293 -0.276783 0.000403
C -0.058537 0.046667 0.000049
O -0.536945 1.151736 0.000096
O -0.861193 -0.977442 -0.000190

344.3, 57.2; 464.3, 138.6; 570.9, 44.4; 776.7, 48.1;
949.4, 8.5; 1195.3, 237.0; 1383.5, 26.4; 1695.1, 420.9;
3839.9, 173.2;

-264.306861418 -264.281301 -264.276571 -264.307840

$CO_3^{\bullet-}(H_2O)$
O 0.104113 -1.130738 0.000072
O 0.266317 1.115660 -0.000086
O -2.490933 0.033567 -0.000120
H -1.770912 -0.621309 -0.000046
H -1.963427 0.840439 -0.000158
C 0.739114 -0.068244 0.000039
O 2.032960 0.005302 0.000131

30.8, 0.1; 105.9, 3.3; 200.5, 19.1; 307.0, 24.7;
314.6, 133.3; 409.0, 38.7; 582.4, 5.6; 701.6, 173.2;
833.7, 61.8; 982.3, 90.6; 1150.8, 8.6; 1653.3, 573.9;
1703.6, 259.2; 3698.6, 306.1; 3875.6, 62.3;

-340.233963811 -340.196261 -340.188795 -340.227852

$CO_3^{\bullet-}(H_2O)_2$
O 1.037444 1.338095 0.002043
C 0.000070 0.584414 -0.000295
O -1.036647 1.338939 -0.001874
O -0.000360 -0.657157 -0.000877
O 2.826994 -1.065013 -0.000260
H 1.865825 -1.211049 -0.000424
H 2.854274 -0.102981 0.000429
O -2.827403 -1.064730 0.000938
H -1.866211 -1.210838 -0.000130
H -2.854524 -0.102685 0.002137

25.8, 0.0; 34.4, 0.0; 65.3, 1.1; 114.5, 8.8;
172.1, 0.8; 216.1, 22.5; 277.9, 0.0; 279.5, 70.4;
327.7, 125.4; 360.1, 126.6; 507.3, 4.7; 574.2, 6.6;
667.3, 0.2; 677.3, 338.2; 826.0, 85.2; 1020.3, 125.3;
1126.6, 1.3; 1668.3, 663.9; 1680.0, 482.6; 1707.4, 18.5;
3710.9, 598.4; 3720.6, 26.6; 3899.6, 0.6; 3900.7, 78.3;

-416.678433693 -416.615648 -416.605056 -416.652638

Structure 3
C -2.376575 0.298735 0.039155
O -3.618512 0.372414 -0.153236
O -1.512029 0.547819 -0.872668
O -2.127201 -0.029073 1.227981
N 1.286838 -0.863249 -0.088719
O 2.464700 -1.025259 0.221308
O 0.517658 -1.789185 -0.291594
O 0.852326 0.343864 -0.204461
H -0.505504 0.399080 -0.556585
O 3.398732 1.740414 0.157084
H 2.449815 1.775059 -0.011635
H 3.501870 0.788240 0.278996

20.7, 1.6; 29.0, 1.0; 43.7, 0.5; 51.8, 1.0;
79.5, 15.3; 112.8, 0.5; 146.2, 38.4; 175.3, 16.9;
188.9, 13.4; 274.2, 0.6; 290.1, 132.9; 570.1, 31.6;
581.2, 145.5; 618.5, 217.7; 741.9, 3.4; 765.3, 61.1;
794.1, 35.6; 852.8, 16.1; 1031.4, 125.0; 1102.7, 192.2;
1120.8, 14.9; 1257.3, 39.5; 1372.9, 1247.8; 1464.2, 58.3;
1607.0, 925.7; 1667.8, 862.7; 1695.2, 79.0; 2146.0,
2588.8;
3844.0, 183.5; 3884.6, 78.4;

-621.144916195 -621.079920 -621.067543 -621.121980

Structure 4
O 2.046801 -1.118002 0.467808
C 2.647241 -0.310748 -0.282025
O 3.764613 -0.755064 -0.843448
O 2.369750 0.856563 -0.590353
O -0.031986 -0.257888 1.473477
H 0.850235 -0.667567 1.038080
H 0.008855 0.720798 1.267911
O 0.173732 2.158161 0.490214
H -0.590834 1.985494 -0.077671
H 0.960493 1.896758 -0.023512
N -2.684731 -0.264424 -0.323144
O -3.707001 -0.579301 -0.902688
O -2.176509 0.861408 -0.443607
O -2.114822 -1.115229 0.439864
H -0.915689 -0.625212 1.019214

25.7, 0.1; 30.7, 0.8; 59.9, 0.9; 62.2, 1.0;
88.6, 2.1; 101.0, 0.2; 119.8, 2.2; 158.7, 2.3;
181.8, 6.2; 256.1, 52.7; 296.5, 411.1; 304.2, 35.0;
401.5, 14.5; 470.3, 127.0; 591.4, 215.7; 650.6, 122.9;
716.8, 73.8; 732.7, 16.6; 766.2, 41.8; 826.8, 31.6;
857.7, 14.8; 940.9, 113.8; 959.0, 82.8; 993.9, 32.1;
1063.1, 5.7; 1126.4, 160.2; 1348.1, 490.1; 1366.3, 214.7;
1405.8, 514.2; 1590.8, 924.7; 1629.8, 1332.7; 1650.0,
56.5;
1720.0, 40.6; 1805.6, 31.0; 2039.9, 3792.9; 2321.5,
1227.2;
3114.7, 818.1; 3650.0, 679.0; 3818.7, 439.7;

-697.590864367 -697.499182 -697.485797 -697.541866